Article

Cell Reports

Manipulating TLR Signaling Increases the Anti-tumor T Cell Response Induced by Viral Cancer Therapies

Graphical Abstract

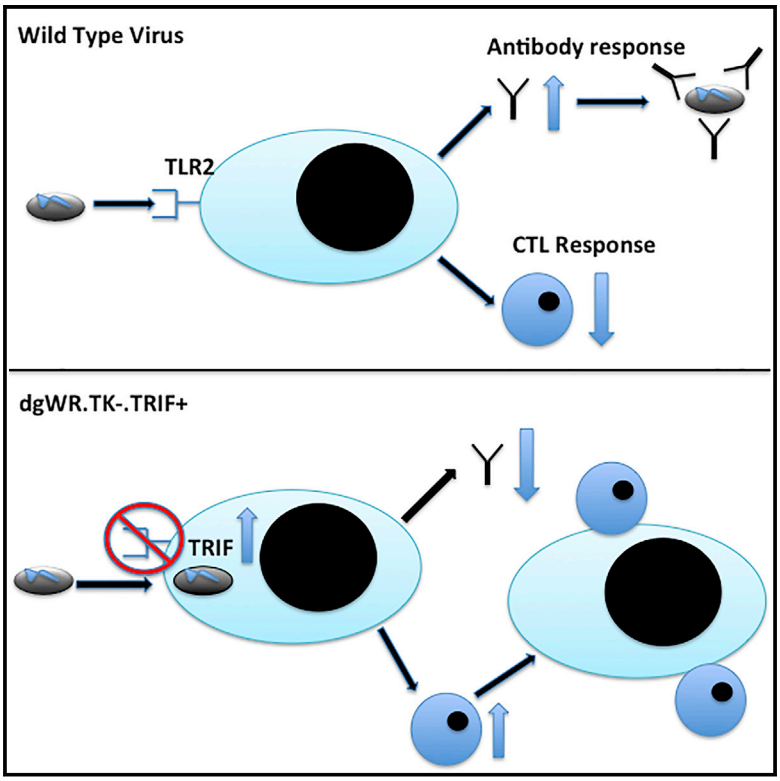

Highlights

- Vaccinia surface deglycosylation reduces TLR2 activation and antibody production
- Vaccinia surface deglycosylation protects against a neutralizing antibody
- Vaccinia TRIF expression induces an increased CTL response
- Deglycosylation and TRIF expression enhances oncolytic vaccinia therapeutic effects

Authors

Juan J. Rojas, Padma Sampath, Braulio Bonilla, Alexandra Ashley, Weizhou Hou, Daniel Byrd, Steve H. Thorne

Correspondence

thornesh@upmc.edu

In Brief

Rojas et al. describe an oncolytic virus containing a combination of surface modification and transgene expression designed to manipulate how the virus activates TLR-signaling pathways. The modified virus induces increased anti-tumor T cell responses and a reduced anti-viral antibody response.

Rojas et al., 2016, Cell Reports *15*, 1–10
April 12, 2016 ©2016 The Authors
http://dx.doi.org/10.1016/j.celrep.2016.03.017

CellPress

Please cite this article in press as: Rojas et al., Manipulating TLR Signaling Increases the Anti-tumor T Cell Response Induced by Viral Cancer Therapies, Cell Reports (2016), http://dx.doi.org/10.1016/j.celrep.2016.03.017

Cell Reports
Article

OPEN ACCESS
CellPress

Manipulating TLR Signaling Increases the Anti-tumor T Cell Response Induced by Viral Cancer Therapies

Juan J. Rojas,[1] Padma Sampath,[1] Braulio Bonilla,[1] Alexandra Ashley,[1] Weizhou Hou,[1] Daniel Byrd,[1] and Steve H. Thorne[1,2,*]
[1]Department of Cell Biology, University of Pittsburgh Cancer Institute, University of Pittsburgh, Pittsburgh, PA 15213, USA
[2]Department of Immunology, University of Pittsburgh, Pittsburgh, PA 15213, USA
*Correspondence: thornesh@upmc.edu
http://dx.doi.org/10.1016/j.celrep.2016.03.017

SUMMARY

The immune response plays a key role in enhancing the therapeutic activity of oncolytic virotherapies. However, to date, investigators have relied on inherent interactions between the virus and the immune system, often coupled to the expression of a single cytokine transgene. Recently, the importance of TLR activation in mediating adaptive immunity has been demonstrated. We therefore sought to influence the type and level of immune response raised after oncolytic vaccinia therapy through manipulation of TLR signaling. Vaccinia naturally activates TLR2, associated with an antibody response, whereas a CTL response is associated with TLR3-TRIF-signaling pathways. We manipulated TLR signaling by vaccinia through deglycosylation of the viral particle to block TLR2 activation and expression of a TRIF transgene. The resulting vector displayed greatly reduced production of anti-viral neutralizing antibody as well as an increased anti-tumor CTL response. Delivery in both naive and pre-treated mice was enhanced and immunotherapeutic activity dramatically improved.

INTRODUCTION

Viral vectors engineered to display tumor selectivity in their replication were first tested clinically as cancer therapies almost 20 years ago (Kirn et al., 1997, 1998; Ganly et al., 2000; Khuri et al., 2000), and although clinical responses were reported, it has become clear that directly lytic viral replication is rarely sufficient to eradicate large tumors or metastatic disease. More recently, the combination of faster-replicating vectors and expression of cytokine (granulocyte macrophage colony-stimulating factor [GM-CSF]) transgenes have resulted in improved clinical responses (Schmidt, 2011; Park et al., 2008; Heo et al., 2013; Andtbacka et al., 2013), and the very real potential for oncolytic viral therapies to effectively treat cancer patients in the clinic has become apparent. These clinical advances highlighted the critical role the immune response can play in the successful application of this platform. Tumor-selective viral replication leads to localized acute inflammation, helps direct the immune response toward the tumor, and transiently overcomes tumor-mediated immunosuppression. Meanwhile, lysis of tumor cells releases relevant tumor antigens and associated danger molecules, resulting in priming of anti-tumor immunity and in situ vaccination. However, to date, this immunotherapeutic activity has relied on the viral vector's naturally evolved interactions with the host immune response, often boosted by the expression of a single cytokine transgene.

Concurrent advances in the development of tumor vaccines have elucidated the advantages of a robust cytolytic T-lymphocyte (CTL) response in the successful treatment of cancer (Okada et al., 2011; June, 2007; Porter et al., 2011; Rosenberg, 2011; Rosenberg et al., 2011). In particular, adjuvant use of certain TLR ligands such as PolyI:C (Zhu et al., 2010; Trumpfheller et al., 2008), which binds TLR3 and activates MyD88-independent signaling pathways, have been found to result in production of increased numbers of CTLs.

Vaccinia virus forms the basis of several of the most-promising oncolytic viral therapies currently in the clinic and has been shown to naturally activate TLR2 as the earliest step in the immune response post-systemic delivery. Infection in TLR2$^{-/-}$ mice resulted in significant reduction in subsequent levels of circulating anti-viral neutralizing antibody (O'Gorman et al., 2010). Because anti-viral neutralizing antibody limits the spread and systemic delivery of oncolytic viral therapies, we sought to ablate this interaction. TLR2 is a cell-surface receptor, meaning that viral binding to TLR2 occurs prior to infection of the target cell, and so prevention of binding to this receptor required an approach involving modification of the viral particle itself.

In order to reinforce this effect, and to further switch the type of immune response elicited after oncolytic virus (OV) therapy toward the potentially more-beneficial Th1 arm, we concurrently enhanced activation of TRIF-mediated signaling pathways downstream of TLR3. Vectors engineered to both reduce TLR2 binding and to enhance TRIF signaling displayed a robust switch in the type of adaptive immune response produced, with a significantly reduced humoral response and enhanced CTL response, as well as showing greatly enhanced therapeutic activity. The effects of altering activation profiles of TLR-signaling pathways on

This is an open access article under the CC BY-NC-ND license (http://creativecommons.org/licenses/by-nc-nd/4.0/).
CELREP 2572

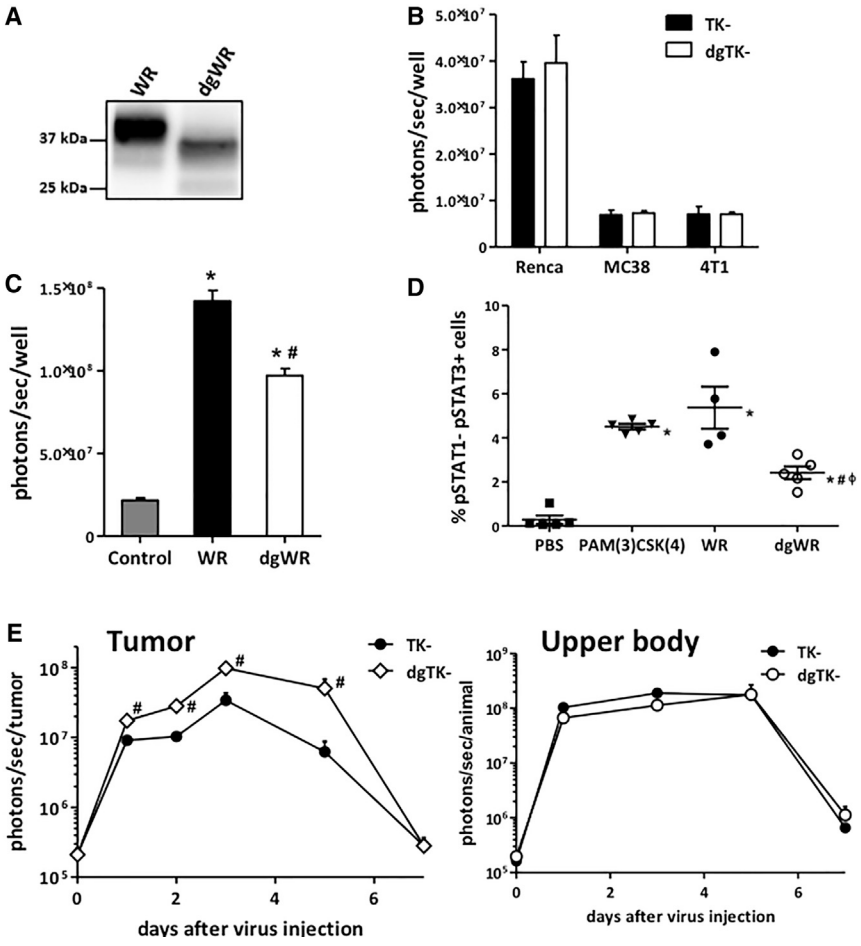

Figure 1. Deglycosylation of Vaccinia Virus Envelope

(A) Immunoblot showing deglycosylation of vaccinia virus envelope protein B5R. Purified WR (wild-type strain WR) and dgWR (deglycosylated) viruses were disrupted and blotted using an anti-B5R antibody. Decrease in protein weight corresponds to deglycosylation of the B5R protein.

(B) Deglycosylation of virus envelope has no effect on vaccinia virus infectivity. Different mouse tumor cell lines were infected with TK− (strain WR with a deletion of the viral thymidine kinase gene) or its deglycosylated version at an MOI of 1, and viral luciferase expression was measured 3 hr after infection by bioluminescence imaging. Mean values + SD of three independent experiments are plotted.

(C) Deglycosylation reduces TLR2 activation in vitro. 293 cells expressing mouse TLR2 were transfected with pNiFty (TLR-signaling reporter plasmid). Twenty-four hours after transfection, cells were infected at an MOI of 1 with WR or dgWR, and TLR2 activation was quantified 24 hr after infection by bioluminescence imaging. Means + SD of two independent experiments (performed in quadruplicate) are depicted.

(D) STAT3 phosphorylation is depleted in splenic lymphocytes of mice injected with deglycosylated vaccinia. C57/BL6 mice were injected intravenously with 1×10^7 plaque-forming units (PFUs) of WR or dgWR, and 1 hr after injection, spleens were excised, dissociated, and prepared for intracellular analysis. Percentage of $pSTAT1^{-}pSTAT3^{+}$ lymphocytes was determined by flow cytometry. PBS and PAM(3)CSK(4) were used as controls. Values of individual mice and means ± SEM of the different treatments are plotted.

(E) Deglycosylation of vaccinia virus (TK−) envelope selectively increases viral gene expression from tumors in vivo. Balb/c mice harboring subcutaneous tumors of Renca cells (mouse renal adenocarcinoma) were randomized and injected with a single intravenous dose of 1×10^8 PFUs per mouse of TK− or dgTK− (both expressing firefly luciferase). Kinetics of viral gene expression from within the tumor (left) or for the upper body (lungs, spleen, and liver signal; right) was monitored by bioluminescence imaging of viral luciferase expression. Mean values of 12 or 13 animals + SD are plotted. *p < 0.05 compared with PBS or control; #p < 0.05 compared with TK− or WR group; ϕp < 0.05 compared with PAM(3)CSK(4) group.

the induction of anti-tumor CTL and anti-viral neutralizing antibody were explored along with the additional beneficial effects on viral systemic delivery to the tumor in single- or repeat-delivery regimens.

RESULTS

Reduction of Vaccinia Binding to TLR2

In initial experiments, we looked to reduce or ablate vaccinia binding to TLR2 in order to reduce MyD88 signaling that we had previously associated with induction of anti-viral neutralizing antibody. It was determined that multiple vaccinia surface proteins were capable of binding and activating this receptor, either as a TLR2 homodimer or a TLR2:6 heterodimer (Figure S1), making genetic modification of the virus complex. Instead, because TLR2 ligands are primarily glycoproteins, we looked to treat the viral particle itself with a mix of deglycosylating enzymes in order to cleave sugars from the viral surface. Successful deglycosylation was confirmed through immunoblot analysis of the viral B5R protein (Figures 1A and S2A). Interestingly, there was no loss of infectivity of tumor cell lines after deglycosylation of the viral particle (Figure 1B; TK− represents vaccinia strain WR with a thymidine kinase deletion and luciferase expression, used as a model oncolytic virus; dgTK− represents deglycosylated TK−); however, activation of pathways downstream of TLR2 binding were significantly reduced both in vitro (reduced necrosis factor κB [NF-κB] activation) and in vivo (reduced pSTAT3 levels) as a result of viral particle deglycosylation (Figures 1C, 1D, and S2B). Activation was not completely lost, but this was not surprising as MyD88-mediated signaling pathways are common to most TLRs.

However, of particular interest was the observation that viral gene expression from the tumor was significantly increased after systemic delivery of deglycosylated virus in several mouse tumor models (Figures 1E and S2C), as determined by bioluminescence imaging of viral luciferase transgene expression. This increase was evident within 24 hr of systemic delivery and led to a >10-fold increase in viral gene expression in the tumor by

OPEN ACCESS
CellPress

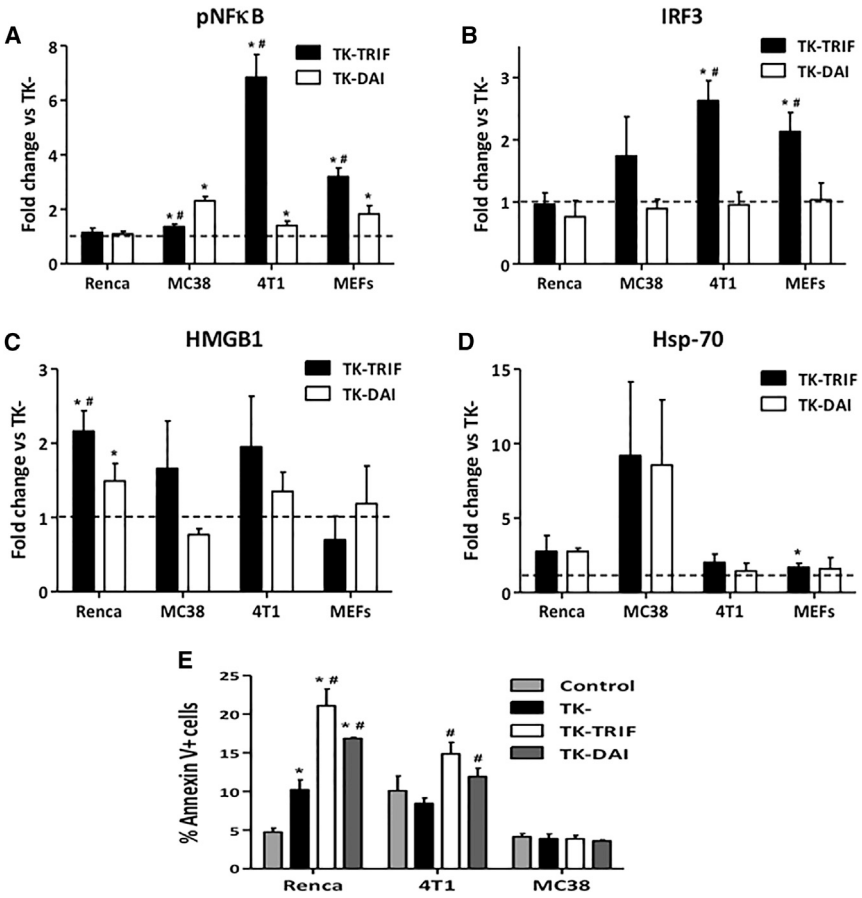

Figure 2. Oncolytic Vaccinia Virus Expressing the Mouse TRIF Protein Increases Activation of TLR-Responding Pathways and the Induction of Necroptosis

(A and B) Activation of NF-κB and IRF3 pathways after infection with TK-TRIF and TK-DAI. ELISA assays were utilized to determine concentrations of pNF-κB (A) and IRF3 (B) in cytoplasmic and nuclear extracts, respectively, of Renca, MC38, 4T1, or MEF cells infected with TK−, TK-TRIF, or TK-DAI at an MOI of 1. Analyses were performed 24 hr after infection. Data were obtained in quadruplicate from two independent experiments and are plotted as fold change versus TK− + SD. Dashed lines indicate TK− activation level.

(C and D) mTRIF expression increases release of danger-associated molecular patterns (DAMPs). ELISA assays were utilized for determining the release of HMGB1 (C) and Hsp-70 (D) after infection with TK−, TK-TRIF, and TK-DAI viruses at an MOI of 1. Quantification was performed 24 hr after infection, and data are depicted as fold change versus TK− + SD, dashed lines indicating TK− release levels.

(E) Percentage of apoptotic cells after infection with TK-TRIF and TK-DAI. A panel of mouse tumor cell lines was infected with the indicated viruses using an MOI of 1. At 48 hr after infection, percentage of necrotic and apoptotic cells were determined by flow cytometry by phosphatidylinositol (PI) and annexin V staining. Two independent experiments were performed, and means + SD are plotted.

day 5 after systemic treatment (relative to TK− control virus). This increase in viral gene expression was restricted to the tumor, with no significant differences seen in bioluminescent signal from other tissues (Figure 1E). Because there were no differences in the ability of the deglycosylated virus to infect or replicate in the same tumor cells in vitro (Figure 1B), and because progeny virus produced after an initial round of replication would be normally glycosylated, it is assumed that the altered viral gene expression pattern is mediated by enhanced delivery to the tumor. TLR2-mediated immune activation (STAT3 phosphorylation) was observed in the majority of cells from multiple lymphoid lineages in the spleen within 15 min of systemic delivery of the virus (O'Gorman et al., 2010). It is likely, therefore, that the reduction in TLR2 activation as a result of viral deglycosylation (Figure 1D) can delay the priming of the immune response until after the initial infection of cells in the tumor, so allowing improved initial delivery and early viral gene expression, leading to enhanced subsequent spread within the tumor.

Expression of TRIF to Enhance CTL Induction

In order to complement the effects of reduced MyD88-pathway signaling, we looked to selectively activate alternate TLR-signaling pathways. In particular, because binding of ligand to TLR3, leading to activation of TRIF pathway signaling, results in the induction of a robust CTL response (Warger et al., 2006; Seya and Matsumoto, 2009), the effects of TRIF expression from vaccinia were examined. Alternatively, DNA-dependent activator of interferon (DAI) activation is also associated with increased CTL induction (Takaoka et al., 2007; Wang et al., 2008), and so the effects of TRIF expression were initially compared to that of DAI through construction and testing of tumor-selective viral vectors expressing each of these innate sensors separately (Figure S3). In initial experiments comparing the effects of TRIF or DAI expression in vitro (Figures 2A, 2B, and S4), both transgenes were found to increase NF-κB activation (Figure 2A), activation of type I interferon (IFN)-signaling pathways (IRF3 expression; Figure 2B), and release of selected cytokines and chemokines relative to our control virus (TK−; Figure S4). However, in all these assays and for multiple cell lines tested, TRIF expression consistently resulted in more-robust innate immune activation than DAI expression. This may be due to vaccinia's inherent activation of the cytoplasmic DNA sensor DAI with limited natural activation of the double-stranded RNA (dsRNA) sensor TLR3.

When TK− and TK-TRIF vectors were compared head to head in vivo through systemic treatment of immunocompetent mice bearing subcutaneous renal cancer (Renca) tumors (Figure 3A), TRIF expression again resulted in increased cytokine and chemokine production within the tumor. However, in vivo, there was a marked preference for enhanced expression of cytokines

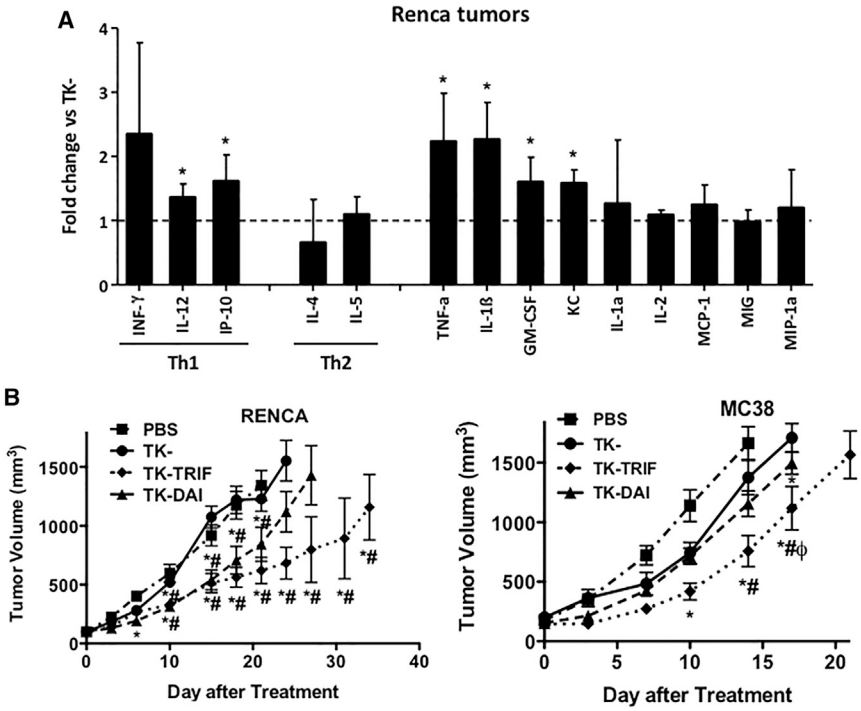

Figure 3. In Vivo Effects of TRIF Expression

(A) In vivo intratumoral concentration of cytokines and chemokines. Balb/c mice with established Renca subcutaneous tumors were randomized and injected with a single intravenous dose of 1×10^8 PFUs per mouse of TK− or TK-TRIF. Four days after injection, tumors were harvested and concentrations of selected cytokines and chemokines were determined in tumor lysates by Luminex or ELISA assays. Fold change versus TK− from four to five mice per group + SD is plotted. Dashed line indicates TK− concentrations. *p < 0.05 compared with TK− group; #p < 0.05 compared with TK-DAI group.

(B) Anti-tumor activity of TK-TRIF and TK-DAI. Renca or MC38 cells were implanted in Balb/c or C57/Bl6 mice, respectively, and mice were injected with PBS or 1×10^8 PFUs of TK−, TK-TRIF, or TK-DAI through the tail vein. Tumor volumes were measured at indicated time points. n = 12–15 mice/group + SE. *p < 0.05 compared with PBS group; #p < 0.05 compared with TK− group; ϕ p < 0.05 compared with TK-DAI group.

involved in the Th1 response (IFN-γ, interleukin-12 [IL-12], and IFN-γ inducible protein 10 [IP-10]) after treatment with TK-TRIF, whereas no such increases were seen in the level of induction of Th2-associated cytokines (IL-4 and IL-5; N.B. IL-6 was below the limits of detection in vivo; Figure 3A). This is in contrast to the cytokine profile produced after infection of Renca cells in vitro, where the Th2 cytokine IL-6 predominated. It is possible that the altered cytokine profiles seen in vitro and in vivo may be at least in part mediated by fibroblasts and other non-tumor cells in the tumor, as murine embryonic fibroblasts (MEFs) in vitro displayed a different profile of cytokine release compared to tumor cell lines with selective increases in IFN-β production (Figure S4). Our recent publication has demonstrated the critical importance of tumor-fibroblast cross talk in the effective application of oncolytic viral therapies (Ilkow et al., 2015).

Neither TRIF nor DAI expression affected viral replication in vitro in two of three cell lines tested; however, both TRIF and DAI reduced viral replication in Renca cells relative to control virus (TK−; Figure S5A). However, despite the reduced viral replication, there was no loss in the tumor cell killing capacity (Figure S5B). The reduced viral replication in Renca cells in vitro was apparently not due to induction of anti-viral immunity, as TRIF (or DAI) expression had the least effect on the immune parameters tested in this cell line (Figures 2A, 2B, and S4). However, a secondary pathway mediated by TRIF acts through RIP3 kinase to induce necroptosis, an immunogenic route of programmed cell death (Kaiser et al., 2013), so the effects of TRIF expression on this pathway were also examined. It was seen that release of known DAMP (danger-associated molecular pattern) molecules (HMGB-1 and Hsp70) were increased in all of the tumor cell lines when infected with virus expressing TRIF; however, this only became significant in Renca cells (Figures 2C and 2D). To further support the hypothesis that the reduced viral replication of TK-TRIF in Renca cells was due to increased immunogenic cell death, we examined the percentage of annexin V+ cells after infection (Figure 2E). It was seen that either TRIF or DAI expression significantly increased the level of annexin V staining in Renca cells. There was also a significant increase in 4T1 cells, but the overall increase was not as dramatic, and there was no effect in MC38 cells. Increased necroptosis and release of DAMPs in Renca cells was therefore coupled to reduce viral replication in vitro.

The anti-tumor effects of TK-TRIF and TK-DAI were also compared to TK− in vivo following systemic delivery of a single dose to two syngeneic mouse tumor models: BALB/c mice bearing Renca tumors or C57/BL6 mice bearing MC38 tumors (Figures 3B and 4A). It was observed that viral gene expression from within the tumor (as determined by bioluminescence imaging of viral luciferase transgene expression) was decreased in both tumor models when TRIF or DAI were expressed (Figure 4A). This is unsurprising, as TRIF and DAI both enhance immune induction mediated by viral infection of these cell lines in vitro (Figures 2A, 2B, and S4). TRIF expression was also found to increase the levels of many Th1-associated cytokines in Renca tumors in vivo (Figure 4B) and was further found to increase the infiltration of both CD3+CD4+ and CD3+CD8+ cells into Renca tumors in vivo (Figure 4C). As such, TRIF expression reduces viral replication in the tumor but enhances immune activation.

Despite the observed reduction in viral gene expression, both TK-TRIF and TK-DAI significantly increased the anti-tumor effect of oncolytic vaccinia therapy (relative to TK−) in Renca or MC38-tumor-bearing mice (Figure 3B). This increased therapeutic effect again demonstrates the advantage of enhancing the immunotherapeutic activity of oncolytic virus strains, even if

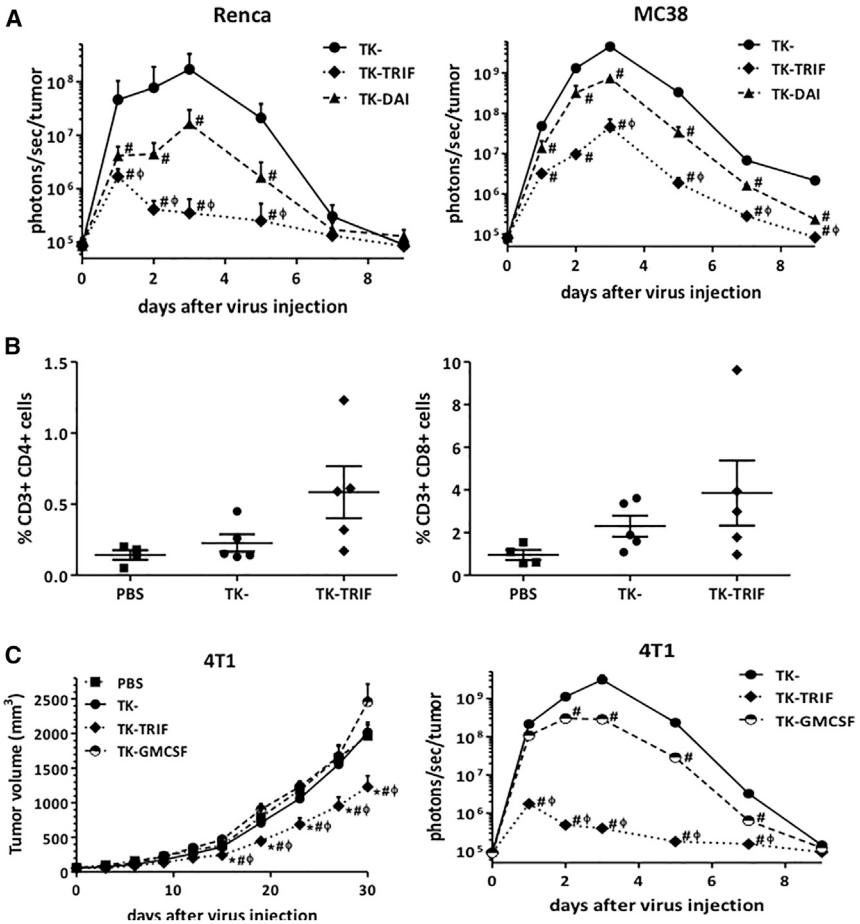

Figure 4. In Vivo Immunotherapeutic Effects of TRIF Expression

(A) Viral gene expression in vivo. Renca or MC38 cells were implanted in Balb/c or C57/Bl6 mice, respectively, and mice were injected with PBS or 1×10^8 PFUs of TK−, TK-TRIF, or TK-DAI through the tail vein. Viral luciferase expression from within the tumors was measured at indicated time points. n = 12–15 mice/group + SE. *, significant $p < 0.05$ compared with PBS group; #, significant $p < 0.05$ compared with TK− group; ϕ, significant $p < 0.05$ compared with TK-DAI group.

(B) Altered T cell repertoire in the tumor after TK− or TK-TRIF injection. Balb/c mice with subcutaneous Renca tumors were treated with a single intravenous injection of PBS or 1×10^8 PFUs/mouse of indicated viruses, and tumors were harvested at day 7 post-virus injection and evaluated for lymphocyte populations by flow cytometry. Percentages of (left) CD3+CD4+ and (right) CD3+CD8+ populations are plotted.

(C) TK-TRIF improves the anti-tumor efficacy compared to TK-GMCSF in a mammary semi-orthotopic model. 4T1 cells were implanted in the mammary fat pad of Balb/c mice, and once the tumor was established, mice were injected with PBS or 1×10^8 PFUs of TK−, TK-TRIF, or TK-GMCSF through the tail vein. (Left) Tumor volumes and (right) viral luciferase expression from within the tumors were measured at indicated time points. n = 12–14 mice/group + SE.

this leads to a reduction in viral replication. In a further mouse tumor model (orthotopically implanted 4T1 breast cancer; Figure 4C), TK-TRIF was compared to TK-mGMCSF (as a mouse equivalent of the clinical JX-594 [Pexa-Vec] viral therapy [Park et al., 2008; Heo et al., 2013]; Jennerex, now part of Silajen) and again demonstrated significantly improved therapeutic effects, despite a reduction in viral gene expression from the tumor (Figure 4C). Of note, in all in vivo experiments, a single intravenous dose of 1×10^8 plaque-forming units (PFUs) was used, a log lower than the dose we have traditionally used. This reduced dose was used to deliberately limit therapeutic activity in order to better delineate the advantages of the vectors developed here. For this reason, some of the control groups display little or no significant activity.

As a result of these data, it was determined to pursue TRIF expression in combination with deglycosylation.

Combining Deglycosylation with TRIF Expression

Because ablation of TLR2 activation may reinforce the immunotherapeutic effects of TRIF expression, we sought to combine the two approaches into a single vector. In initial studies, TK-TRIF virus was deglycosylated as before (dgTK-TRIF), and the anti-viral immune response elicited in mice was compared to TK−, dgTK−, and TK-TRIF (Figures 5A and 5B). It was found that dgTK-TRIF demonstrated a profound switch from Th2 to Th1 immunity as seen with significantly enhanced anti-viral CTL response and significantly reduced anti-viral neutralizing antibody titer. Further, when anti-tumor CTL response was determined in tumor-bearing mice, it was seen that only dgTK-TRIF displayed significantly greater induction of anti-tumor CTL response relative to TK− virus (Figure 5C). This capacity to switch the type of immune response raised by a viral vector has the potential to significantly enhance the therapeutic activity of multiple therapies, including different oncolytic vectors, or for other vaccine approaches.

When viral gene expression from the tumor was followed after systemic delivery to Renca tumors in vivo, it was seen that, although deglycosylation of TK-TRIF did again result in increased viral gene expression in the tumor (relative to TK-TRIF alone), this was not sufficient to restore replication to the levels of the parental vector (TK−; Figure 5D). However, the reduced replication of dgTK-TRIF relative to TK− also provides a significant safety advantage. Viral treatments in naive animals (Figure 5E) demonstrated that dgTK-TRIF treatment resulted in only minor and transient weight loss that was significantly less than seen with the TK− virus. Alternatively, the induction of high numbers of CTL may raise concerns of auto-immunity. This was also examined, and no induction of anti-ssDNA

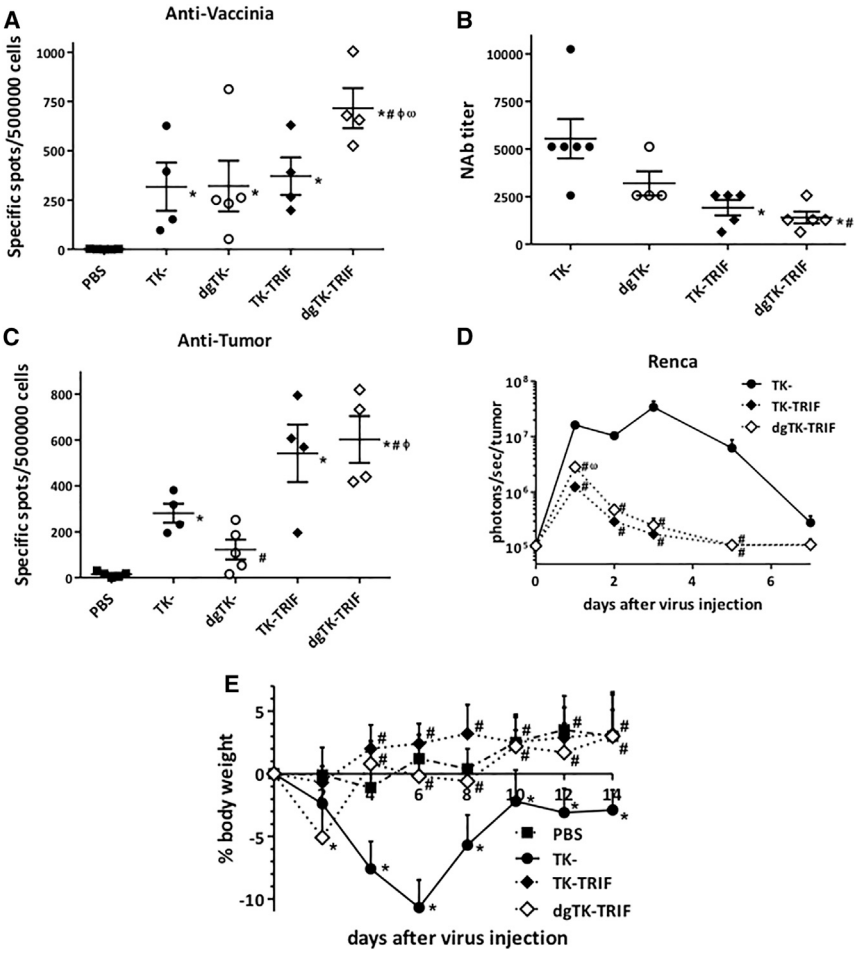

Figure 5. Combination of Envelope Deglycosylation and Mouse TRIF Expression Boosts Anti-tumor Cellular Responses and Enhances Safety

(A) Cellular immune response to vaccinia virus evaluated by IFN-γ ELISpot assay. At day 7, post-virus administration spleens were harvested from mice injected intravenously with 1×10^8 PFUs of indicated viruses or PBS (Balb/c mice bearing Renca tumors) and evaluated for the amount of CTLs recognizing vaccinia virus. Values of individual mice and means ± SEM are depicted.

(B) Serum-neutralizing antibody titers. A neutralizing assay was performed to determine circulating anti-vaccinia antibody levels for mice injected with 1×10^8 PFUs of TK−, dgTK−, TK-TRIF, or dgTK-TRIF. Nabs titers were determined by the highest dilution of serum that resulted in at least 50% inhibition of cell-killing capacity. Values of individual mice and means ± SEM are plotted.

(C) CTL response was measured as in (A), except ELIPSOT was performed against Renca cell lysate.

(D) Viral gene expression in vivo after dgTK-TRIF administration. Renca tumors were implanted in Balb/c mice, and mice were injected with PBS or 1×10^8 PFUs of TK−, TK-TRIF, or dgTK-TRIF through the tail vein. Viral luciferase expression from within the tumors was measured at indicated time points. n = 12–14 mice/group + SE.

(E) Body weight change after intravenous viral administration. Balb/c mice were injected intravenously with 1×10^8 PFUs per mouse of TK−, TK-TRIF, or dgTK-TRIF. PBS administration was used in the control group. TK-injected mice presented more than 10% reduction in body weight at day 6 after virus injection, whereas TK-TRIF- and dgTK-TRIF-injected mice presented a similar weight profile as those injected with PBS.

antibodies or pathology in normal tissues was seen (Figure S6), indicating dgTK-TRIF did not cause auto-immunity.

Critically, dgTK-TRIF displayed significantly enhanced therapeutic activity over either the dgTK− or TK-TRIF vectors in both the Renca and the MC38 tumor models (again after a single intravenous [i.v.] treatment; Figure 6A). Because JX-594 (Pexa-Vec) represents the leading clinical oncolytic vaccinia and has reached primary endpoints in randomized testing, the therapeutic effects of dgTK-TRIF were compared to TK-mGMCSF (mouse equivalent of JX-594; Pexa-Vec) in a panel of four different mouse tumor models (Figure 6B). dgTK-TRIF demonstrated significantly enhanced therapeutic activity in all models examined, meaning that dgTK-TRIF demonstrates both increased safety and therapeutic activity relative to the most-promising current clinical oncolytic vaccinia strain.

Repeat Systemic Delivery of dgTK-TRIF

One critical limitation with oncolytic virotherapy is the reduced capability to repeatedly systemically deliver the virus to the tumor once an anti-viral immune response has been raised. In initial testing, it was observed that deglycosylation (dgTK−) protected the viral particle from neutralizing antibody raised against parental vaccinia virus (Figure 7A). Because progeny virus produced after initial delivery of a deglycosylated virus will be normally glycosylated, neutralizing antibody raised after treatment with dgTK− will primarily target the fully glycosylated form. Furthermore, because dgTK-TRIF raises a primarily CTL immune response, with reduced levels of anti-viral neutralizing antibody, this vector should have even further enhanced capacity for repeated systemic delivery to the tumor. This was tested through initial systemic delivery of TK− or dgTK-TRIF, followed by a subsequent delivery (7 days later) of the same viruses. This translated into further increased therapeutic potential. Whereas two systemic treatments with TK− virus (7 days apart) resulted in no additional therapeutic benefit relative to a single delivery, repeat cycles of dgTK-TRIF further and significantly increased therapeutic activity, resulting in seven of ten complete responses in the aggressive mouse tumor model used (Figure 7B).

DISCUSSION

Although some advances have been made in the treatment of cancer over the last 20 years, most therapeutic platforms primarily aim to control the disease rather than achieving durable long-term cures. However, the recent success of several immunotherapies, including blockade of immune checkpoint inhibitors

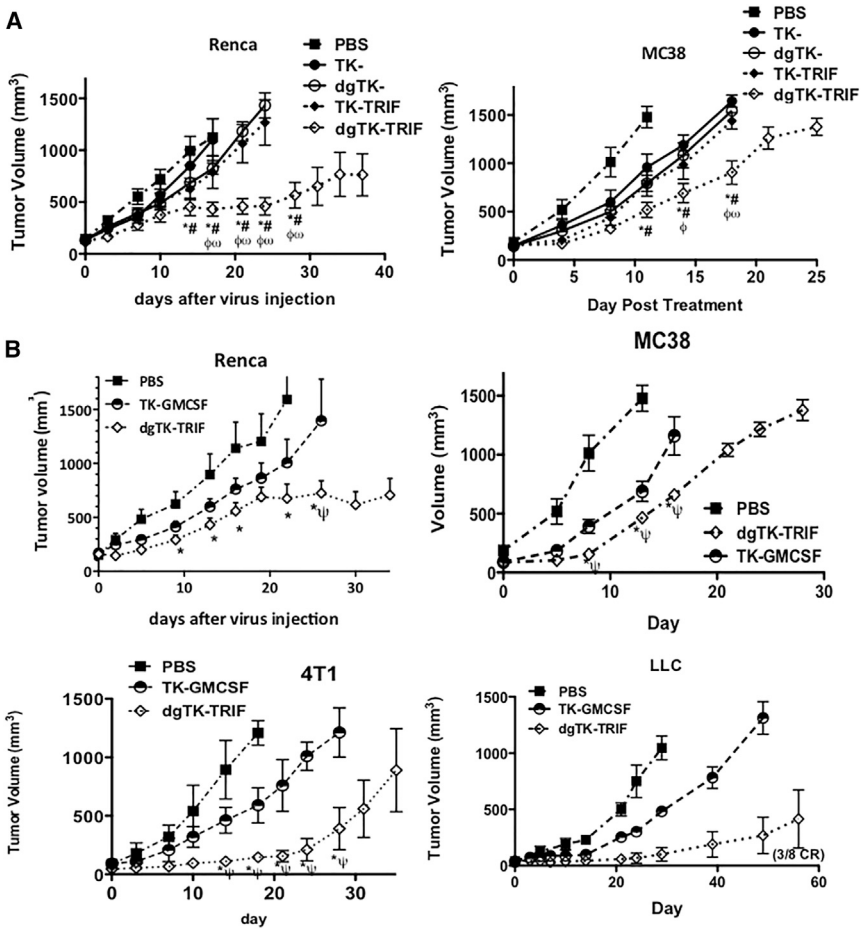

Figure 6. In Vivo Anti-tumor Activity in Different Models

(A) Balb/c-bearing Renca (left) or C57/BL6-bearing MC38 (right) tumors were treated with a single intravenous dose of indicated viruses (1×10^8 PFUs/mouse). Tumor growth was followed by caliper measurements. Means of 12–15 mice per group + SE are depicted.

(B) dgTK-TRIF improves anti-tumor activity compared to TK-mGMCSF. Immunocompetent mice harboring Renca, MC38, Pan02, or 4T1 tumors were injected intravenously with a dose of 1×10^8 PFUs/mouse of TK-mGMCSF or dgTK-TRIF. Relative tumor volume after virus administration is plotted (n = 12–15 mice/group + SE). *p < 0.05 compared with PBS group; Ψp < 0.05 compared with TK-GMCSF group.

(Leach et al., 1996; Topalian et al., 2012), has demonstrated the potential for harnessing the immune response to both clear minimal residual disease and to maintain long-term immune surveillance.

Another platform that has begun to recapitulate pre-clinical success in a clinical setting is that of oncolytic viral therapy, primarily driven by vectors that express GM-CSF to stimulate the immune response and so create a secondary anti-tumor mechanism (Park et al., 2008; Heo et al., 2013). The clinical demonstration that the immune response raised by oncolytic viruses can be critical for their therapeutic success has been coupled to pre-clinical demonstrations that these therapies can act as in situ vaccines, cross-priming an adaptive immune response against relevant tumor antigens as a result of their tumor-selective replication. This led us to attempt to logically redesign an oncolytic vaccinia to specifically optimize interactions with the host's immune system.

The resulting dgTK-TRIF vector has multiple unique features, demonstrates significant therapeutic advantages over the current leading clinical vaccinia vector (JX-594; Pexa-Vec) in pre-clinical models, and provides insight into host-pathogen interactions that could be applied to other vaccination approaches. The fact that dgTK-TRIF displays greatly increased anti-tumor effects despite reduced directly "oncolytic" activity also means that it might be better considered as founding a class of therapies, immuno-oncolytic vectors.

The stripping of sugars from the viral particle provides a unique opportunity to delay immune activation and influence the immune response pathways before the vector has even reached a target cell. Our previous studies have demonstrated that vaccinia binding to TLR2 leads to rapid STAT3 phosphorylation and increased neutralizing antibody production (O'Gorman et al., 2010). We have therefore altered the viral particle itself in order to influence the type of immune response raised.

In addition, combining this reduction in TLR2 (MyD88-dependent) pathway activation with TRIF expression resulted in a clear switching of the polarity of the immune response from a Th2 to a primarily Th1 arm. Through manipulation of TLR-signaling pathways, we have demonstrated such a switch in the immune response raised against a microbe. The resulting vector not only demonstrates clear therapeutic benefits over control and current clinical vectors but also the reduced overall viral replication and no induction of auto-immunity results in significantly reduced toxicity, meaning the vector also has a favorable safety profile.

This switch from a Th2- to a Th1-skewed immune response coupled with enhanced safety also indicates possible uses of this vector beyond the field of oncology, as the basis for a safe and antigen-expressing vaccine for use against a variety of diseases where a primarily CTL response is desired. Vaccinia-based vaccines are being developed against diverse diseases, including HIV (Essajee and Kaufman, 2004), Ebola (Geisbert et al., 2002), and Plasmodium (Ockenhouse et al., 1998) infections, and modifications described here may generate more-effective protective immunity.

Finally, because (1) deglycosylation protects the virus against neutralizing antibody targeting the parental virus; (2) progeny virus will be fully glycosylated, so anti-viral immunity will primarily

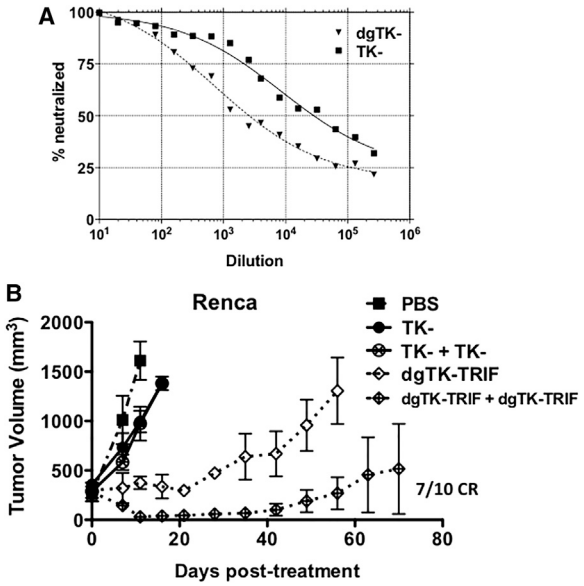

Figure 7. dgTK-TRIF Displays Enhanced Systemic Delivery and Therapeutic Activity during Repeat Cycles of Treatment

(A) Deglycosylated virus is resistant to anti-vaccinia neutralizing antibody. 1×10^3 PFUs of TK− and deglycosylated TK− were mixed with limiting dilutions of VIG (vaccinia immunoglobulin G [IgG]) for 30 min before addition to a fresh cell layer and luciferase reading taken 24 hr later (uninfected cells and virus with no VIG were used to define 0% and 100% neutralization).

(B) Enhanced therapeutic activity of repeated delivery of deglycosylated virus. Mice (BALB/c-bearing Renca tumors) were treated i.v. with 1×10^8 PFUs of indicated virus. After 7 days, mice were treated with a second dose of the same viruses. Tumors were measured over time (n = 12–15 per group). dgTK-TRIF displayed significantly enhanced therapeutic activity ($p < 0.05$) relative to all other treatment groups from day 10 onward.

be raised against the glycosylated form; and (3) dgTK-TRIF produces significantly less anti-viral antibody as a result of the Th2 to Th1 switch, this vector retains systemic delivery potential through repeat cycles of treatment. This provides the potential to overcome one of the major current limitations of oncolytic viral therapy, a limited capacity for repeat delivery. In addition, the capacity to successfully deliver a second dose of therapy, even after an anti-viral immune response has been raised, creates the potential for enhancing the immune response raised through prime-boost effects, something that has traditionally required the use of multiple serologically distinct viruses to achieve.

Overall, the data clearly demonstrate the potential of optimizing the immune response raised by oncolytic viral vectors as a means to enhance therapeutic activity, and we believe this will form the basis of a powerful cancer treatment approach. The dgTK-TRIF vector described here represents a promising cancer treatment approach that will be translated into a clinical setting.

EXPERIMENTAL PROCEDURES

Cell Culture and Transfection

HeLa (human cervix adenocarcinoma), Bsc-1 (green monkey normal kidney cells), 143B (human osteosarcoma), CV-1 (green monkey kidney fibroblasts), Renca (murine renal adenocarcinoma), Pan02 (murine pancreatic cancer), and 4T1 (murine breast cancer) cell lines were obtained from the American Type Culture Collection. 293-mTLR2 cells were purchased from InvivoGen. MC38 (murine colon adenocarcinoma) and MEFs cell lines were, respectively, a kind gift from Dr. David Bartlett and Dr. Robert Sobol (University of Pittsburgh Cancer Institute). 293-hTLR2 and 293-hTLR2-hTLR6 were a gift from Dr. Saumen Sarkar (University of Pittsburgh Cancer Institute). All cell lines were maintained in recommended culture media containing 5%–10% fetal bovine serum and antibiotics at 37°C, 5% CO_2.

pNiFty (TLR-signaling reporter plasmid-luciferase) was obtained from InvivoGen and transfected to 293/mTLR2 cells using FuGENE HD transfection reagent (Promega).

Viruses

Western Reserve (WR) vaccinia strain was obtained from BEI Resources, and all recombinant vaccinia viruses used or constructed for this work are based on this strain. TK− vaccinia virus and its derivatives (TK-TRIF and TK-DAI) contain a deletion in the viral thymidine kinase gene (*tk*−) and express the firefly luciferase gene from the synthetic vaccinia promoter pE/L (Chakrabarti et al., 1997). Luciferase expression from this promoter allows monitoring of bioluminescence as an indicator of viral replication (Chen et al., 2013). In strains TK-TRIF and TK-DAI, murine TRIF (TICAM1) and murine DAI (DLM-1/ZBP1), respectively, are expressed from the early/late vaccinia promoter p7.5 and cloned into the locus of the viral thymidine kinase gene (Figure S2A). Viruses were titered by plaque assay on BSC-1 cell line and manufactured and purified as previously described for in vivo use (Sampath et al., 2013).

For deglycosylation of viruses, an enzymatic deglycosylation kit was used (Glycopro; Prozyme). N-linked and simple O-linked glycans are removed from the viral envelope using a cocktail of N- and O-glycanases and sialidase A.

Protein Analysis

To analyze the deglycosylation of vaccinia virus surface proteins, 1×10^6 PFUs of WR or dgWR were disrupted by mixing with Laemmli buffer and incubating at 65°C for 10 min. After separation with SDS-PAGE and transfer to a nitrocellulose membrane, membranes were dyed with Coomassie blue for total protein staining or immunoblotted using an anti-B5R primary antibody (mouse; BEI Resources) and a polyclonal anti-mouse conjugated with horseradish peroxidase (HRP) (goat; Thermo Scientific).

For evaluating DAI expression, cell cultures seeded in 6-well plates were infected at an MOI of 5 (PFUs/cell), and 24 hr after infection, whole-cell protein extracts were obtained by incubation in cell lysis buffer (Cell Signaling Technology) for 1 hr at 4°C. Clarified samples (15 μg/lane) were separated on a 10% SDS-PAGE gel and transferred to a nitrocellulose membrane. Mouse DAI protein was detected by immunoblotting membranes using a polyclonal anti-DAI primary antibody (rabbit; Abcam) and a polyclonal anti-rabbit antibody conjugated to HRP (goat; Thermo Scientific). A mouse monoclonal anti-β actin antibody (Santa Cruz Biotechnologies) and a peroxidase-conjugated anti-mouse antibody (goat; Thermo Scientific) were used for immunoblotting of β-actin as a loading control.

Evaluation of TLR2 activation by vaccinia proteins utilized recombinant proteins expressed in eukaryotic cells provided placed on 293 cell lines transfected to express hTLR2 or hTLR2 and hTLR6 and activation assayed using the pNiFty plasmid in a luciferase assay; an IRF3 promoter-driven luciferase was used as a control.

Mouse Models

All animal studies were approved by the University of Pittsburgh Institutional Animal Care and Use Committee. BALB/c and C57/BL6 female mice (6–8 weeks old) were purchased from The Jackson Laboratory. For Renca or MC38 tumor isografts, tumor cell lines were implanted subcutaneously at 5×10^5 cells per mouse into BALB/c or C57/BL6 mice, respectively. For 4T1, a semi-orthotopic model was used with 2×10^5 4T1 cells implanted into the fat pad of the mammary gland of BALB/c female mice. When tumor reached ~50–100 mm^3, oncolytic vaccinia viruses were administrated intravenously into the tail vein at doses of 1×10^9PFUs/mouse, unless otherwise stated. Tumor volume was monitored by caliper measurement and was defined by the equation $V(mm^3) = \pi/6 \times W^2 \times L$, where W and L are the width

and the length of the tumor, respectively. Data are expressed as tumor size relative to the beginning of the therapy, which was set as 100%. For Kaplan-Meier survival curves, endpoint was established at $\geq$750 mm^3. The survival curves obtained were compared for the different treatments. Animals whose tumor size never achieved the threshold were included as right-censored information.

For the auto-immunity assays, mice were sacrificed 21 days after treatment and serum collected for determination of anti-single-stranded DNA (ssDNA) antibody levels and tissues (liver, lung, kidney, and spleen) collected for H&E analysis.

Bioluminescence Imaging

Viral gene expression was determined through bioluminescence imaging of luciferase expression both in vitro and in vivo. For cultured cells, 10 μl of 30 mg/ml D-luciferin (GoldBio) was added to 1 ml of culture media. For animal models, a dose of 4.5 mg of D-luciferin was injected intraperitoneally per mouse before imaging. An IVIS2000 model (PerkinElmer) was used for the imaging, and images were analyzed with LivingImage software (PerkinElmer).

Flow Cytometry

For testing STAT1 and STAT3 phosphorylation in splenocytes, spleens were harvested from C57/BL6 mice 1 hr after injection of indicated viruses and splenocytes were isolated, fixated in 1.6% paraformaldehyde (PFA), and permeabilized with methanol. Two-color intracellular immunostaining analyses were performed using a LSRFortessa Flow Cytometer (BD Biosciences). Splenocytes were stained using PacificBlue anti-mouse pSTAT1 and Alexa Fluor 647 anti-mouse pSTAT3 antibodies (BD Biosciences).

For evaluation of immune populations in tumors, tumors were harvested from mice treated as indicated and mechanically disaggregated and digested with triple-enzyme mixture (collagenase type IV, DNase type IV, and hyaluronidase type V; Sigma-Aldrich). Four-color cell surface immunostaining analyses were performed using a Gallios Flow Cytometer (Beckman Coulter Genomics). Tumor-disaggregated cells were stained using phycoerythrin (PE)-Cy7 anti-mouse CD3 (BD Biosciences), fluorescein isothiocyanate (FITC) anti-mouse CD4, PerCP-Cy5.5 anti-mouse CD8, and PE anti-mouse CD25 (eBioscience).

For apoptosis/necrosis evaluation of cell lines, cells were infected with an MOI of 1 with indicated viruses and stained using an Annexin V-FITC Apoptosis Detection Kit (Abcam) 48 hr after infection. Analyses were performed using an Accuri C6 Flow Cytometer (BD Biosciences).

ELISAs

Different ELISA kits were used for determining protein concentrations in supernatant, cell extracts, or nuclear extracts of cells infected at an MOI of 1 (PFU/cell) with indicated viruses. Mouse TRIF, HMGB1, and IRF3 ELISA kits were purchased from Antibodies-online, and mouse NFκB pathway activation ELISA kit and HSP-70 ELISA kit were purchased from eBioscience and Abcam, respectively. Mouse ssDNA ELISA was purchased from Alpha Diagnostics.

For mouse IFN-γ concentrations in tumor lysates, an IFN-γ ELISA kit (R&D Systems) was used. Tumors harvested from mice treated as indicated were homogenized using Lysing Matrix D tubes and a FastPrep-24 instrument (MP Biomedicals).

Luminex

Evaluation of the concentration of cytokines and chemokines in cell culture supernatants and tumor lysates by Luminex assay was performed by The Luminex Core Facility of The University of Pittsburgh Cancer Institute. For cell culture supernatants, a Miliplex Mouse Cytokine Panel (5-plex) Kit from Millipore and a Mouse 2-plex assay Kit from Panomics were used. For tumor lysates, a Cytokine Mouse 20-plex Panel Kit from Invitrogen was used for determining concentrations in tumors harvested at day 4 after vaccinia virus administration. Tumors were homogenized using Lysing Matrix D tubes and a FastPrep-24 instrument, as before indicated.

Viral Production and Cytotoxicity Assays

2×10^5 cells were seeded in 24-well plates and infected at an MOI of 1 (PFU/cell) with indicated vaccinia viruses. Four hours after infection, cultures were washed twice with PBS and incubated in fresh virus-free medium. At indicated time points after infection, cultures were harvested and frozen-thawed three times to obtain the cell extract (CE). Viral titers were determined by plaque assay on BSC-1 cells.

Cytotoxicity assay was performed by seeding 2×10^4 cells per well in 96-well plates in DMEM with 5% FBS. Cells were infected with serial dilutions starting at an MOI of 75, and at day 4 post-infection, plates were washed with PBS and absorbance was quantified after staining cultures using a nonradioactive cell proliferation assay kit (Promega). Inhibitory concentration 50% (IC_{50}) values (PFUs per cell required to produce 50% inhibition) were estimated from dose-response curves by standard nonlinear regression, using an adapted Hill equation.

Neutralizing Antibody Assay

Antibody-containing serum was obtained from mice treated as indicated at day 14 after virus injection and incubated for 30 min at 56°C to inactivate the complement. Serial dilutions (in triplicate) of the serum, starting at 1/20, were used to neutralize 1,000 PFUs of TK− vaccinia virus. 2×10^4 HeLa cells were plated per well in 96-well and infected with serum-virus mix. At day 4 post-infection, plates were washed with PBS and absorbance was quantified after staining cultures using a nonradioactive cell proliferation assay kit (Promega). NAb titer was determined as the lowest dilution able to neutralize 50% of virus cell killing capacity.

IFN-γ ELISPOTs

For ELISPOT assays, splenocytes were prepared from mice bearing Renca tumors treated as indicated. Splenocytes were mixed with tumor cells or splenocytes previously infected with UV-inactivated vaccinia virus at 5:1 ratio. Naive splenocytes from each mouse were used as control. 96-well membrane filter plates (EMD Millipore) coated with 15 μg/ml of monoclonal anti-mouse IFN-γ antibody AN18 (Mabtech) were used for the assays. Cells were maintained for 48 hr at 37°C, and spots were detected using 1 μg/ml of biotinylated anti-mouse INF-γ antibody R4-6A2-biotin (Mabtech). Plates were developed using an ABC kit and an AEC substrate kit for peroxidase (Vector Laboratories). Specific spots were counted and analyzed using an ImmunoSpot Analyzer and software (CTL).

Statistical Analysis

Standard Student's t tests (two-tailed) were used throughout this work, except for comparison of survival curves, where a log rank was used. In all cases, significance was achieved if $p < 0.05$.

SUPPLEMENTAL INFORMATION

Supplemental Information includes six figures and can be found with this article online at http://dx.doi.org/10.1016/j.celrep.2016.03.017.

AUTHOR CONTRIBUTIONS

J.J.R. performed the majority of the experiments described in this work. P.S. ran some of the original deglycosylation work, and A.A. ran some of the TLR activation pathway experiments. D.B., B.B., and W.H. assisted, primarily with mouse work. S.H.T. oversaw the project and wrote the manuscript.

CONFLICTS OF INTEREST

S.H.T. has a financial interest in Western Oncolytics, which has licensed the technology described herein.

ACKNOWLEDGMENTS

This work was supported by R01CA140215 and R01 CA178766, whereas core facilities funded under the CCSG (P30CA047904) were used, including In Vivo Imaging, Small Animal, and Flow cytometry facilities. S.H.T. has a financial interest in Western Oncolytics that has licensed this technology.

Received: August 4, 2015
Revised: January 8, 2016
Accepted: March 1, 2016
Published: March 31, 2016

REFERENCES

Andtbacka, R.H.I., Collichio, F.A., Amatruda, T., Senzer, N.N., Chesney, J., Delman, K.A., Spitler, L.E., Puzanov, I., Doleman, S., Ye, Y., et al. (2013). OPTiM: A randomized phase III trial of talimogene laherparepvec (T-VEC) versus subcutaneous (SC) granulocyte-macrophage colony-stimulating factor (GM-CSF) for the treatment (tx) of unresected stage IIIB/C and IV melanoma. J. Clin. Oncol. *31*, LBA9008.

Chakrabarti, S., Sisler, J.R., and Moss, B. (1997). Compact, synthetic, vaccinia virus early/late promoter for protein expression. Biotechniques *23*, 1094–1097.

Chen, H., Sampath, P., Hou, W., and Thorne, S.H. (2013). Regulating cytokine function enhances safety and activity of genetic cancer therapies. Mol. Ther. *21*, 167–174.

Essajee, S., and Kaufman, H.L. (2004). Poxvirus vaccines for cancer and HIV therapy. Expert Opin. Biol. Ther. *4*, 575–588.

Ganly, I., Kirn, D., Eckhardt, G., Rodriguez, G.I., Soutar, D.S., Otto, R., Robertson, A.G., Park, O., Gulley, M.L., Heise, C., et al. (2000). A phase I study of Onyx-015, an E1B attenuated adenovirus, administered intratumorally to patients with recurrent head and neck cancer. Clin. Cancer Res. *6*, 798–806.

Geisbert, T.W., Pushko, P., Anderson, K., Smith, J., Davis, K.J., and Jahrling, P.B. (2002). Evaluation in nonhuman primates of vaccines against Ebola virus. Emerg. Infect. Dis. *8*, 503–507.

Heo, J., Reid, T., Ruo, L., Breitbach, C.J., Rose, S., Bloomston, M., Cho, M., Lim, H.Y., Chung, H.C., Kim, C.W., et al. (2013). Randomized dose-finding clinical trial of oncolytic immunotherapeutic vaccinia JX-594 in liver cancer. Nat. Med. *19*, 329–336.

Ilkow, C.S., Marguerie, M., Batenchuk, C., Mayer, J., Ben Neriah, D., Cousineau, S., Falls, T., Jennings, V.A., Boileau, M., Bellamy, D., et al. (2015). Reciprocal cellular cross-talk within the tumor microenvironment promotes oncolytic virus activity. Nat. Med. *21*, 530–536.

June, C.H. (2007). Adoptive T cell therapy for cancer in the clinic. J. Clin. Invest. *117*, 1466–1476.

Kaiser, W.J., Sridharan, H., Huang, C., Mandal, P., Upton, J.W., Gough, P.J., Sehon, C.A., Marquis, R.W., Bertin, J., and Mocarski, E.S. (2013). Toll-like receptor 3-mediated necrosis via TRIF, RIP3, and MLKL. J. Biol. Chem. *288*, 31268–31279.

Khuri, F., Nemunaitis, J., Ganly, I., Gore, M., MacDougal, M., Tannock, I., Kaye, S., Hong, W., and Kirn, D. (2000). A controlled trial of Onyx-015, an E1B gene-deleted adenovirus, in combination with chemotherapy in patients with recurrent head and neck cancer. Nat. Med. *6*, 879–885.

Kirn, D., Ganley, I., Nemunaitis, J., and AL., E. (1997). A phase I clinical trial with ONYX-015 (a selectively replicating adenovirus) administered by intratumoral injection in patients with recurrent head and neck cancer. Cancer Gene Ther. ■ ■ ■, 4.

Kirn, D., Hermiston, T., and McCormick, F. (1998). ONYX-015: clinical data are encouraging. Nat. Med. *4*, 1341–1342.

Leach, D.R., Krummel, M.F., and Allison, J.P. (1996). Enhancement of antitumor immunity by CTLA-4 blockade. Science *271*, 1734–1736.

O'Gorman, W.E., Sampath, P., Simonds, E.F., Sikorski, R., O'Malley, M., Krutzik, P.O., Chen, H., Panchanathan, V., Chaudhri, G., Karupiah, G., et al. (2010). Alternate mechanisms of initial pattern recognition drive differential immune responses to related poxviruses. Cell Host Microbe *8*, 174–185.

Ockenhouse, C.F., Sun, P.F., Lanar, D.E., Wellde, B.T., Hall, B.T., Kester, K., Stoute, J.A., Magill, A., Krzych, U., Farley, L., et al. (1998). Phase I/IIa safety, immunogenicity, and efficacy trial of NYVAC-Pf7, a pox-vectored, multiantigen, multistage vaccine candidate for Plasmodium falciparum malaria. J. Infect. Dis. *177*, 1664–1673.

Okada, H., Kalinski, P., Ueda, R., Hoji, A., Kohanbash, G., Donegan, T.E., Mintz, A.H., Engh, J.A., Bartlett, D.L., Brown, C.K., et al. (2011). Induction of CD8+ T-cell responses against novel glioma-associated antigen peptides and clinical activity by vaccinations with alpha-type 1 polarized dendritic cells and polyinosinic-polycytidylic acid stabilized by lysine and carboxymethylcellulose in patients with recurrent malignant glioma. J. Clin. Oncol. *29*, 330–336.

Park, B.H., Hwang, T., Liu, T.C., Sze, D.Y., Kim, J.S., Kwon, H.C., Oh, S.Y., Han, S.Y., Yoon, J.H., Hong, S.H., et al. (2008). Use of a targeted oncolytic poxvirus, JX-594, in patients with refractory primary or metastatic liver cancer: a phase I trial. Lancet Oncol. *9*, 533–542.

Porter, D.L., Levine, B.L., Kalos, M., Bagg, A., and June, C.H. (2011). Chimeric antigen receptor-modified T cells in chronic lymphoid leukemia. N. Engl. J. Med. *365*, 725–733.

Rosenberg, S.A. (2011). Cell transfer immunotherapy for metastatic solid cancer–what clinicians need to know. Nat. Rev. Clin. Oncol. *8*, 577–585.

Rosenberg, S.A., Yang, J.C., Sherry, R.M., Kammula, U.S., Hughes, M.S., Phan, G.Q., Citrin, D.E., Restifo, N.P., Robbins, P.F., Wunderlich, J.R., et al. (2011). Durable complete responses in heavily pretreated patients with metastatic melanoma using T-cell transfer immunotherapy. Clin. Cancer Res. *17*, 4550–4557.

Sampath, P., Li, J., Hou, W., Chen, H., Bartlett, D.L., and Thorne, S.H. (2013). Crosstalk between immune cell and oncolytic vaccinia therapy enhances tumor trafficking and antitumor effects. Mol. Ther. *21*, 620–628.

Schmidt, C. (2011). Amgen spikes interest in live virus vaccines for hard-to-treat cancers. Nat. Biotechnol. *29*, 295–296.

Seya, T., and Matsumoto, M. (2009). The extrinsic RNA-sensing pathway for adjuvant immunotherapy of cancer. Cancer Immunol. Immunother. *58*, 1175–1184.

Takaoka, A., Wang, Z., Choi, M.K., Yanai, H., Negishi, H., Ban, T., Lu, Y., Miyagishi, M., Kodama, T., Honda, K., et al. (2007). DAI (DLM-1/ZBP1) is a cytosolic DNA sensor and an activator of innate immune response. Nature *448*, 501–505.

Topalian, S.L., Hodi, F.S., Brahmer, J.R., Gettinger, S.N., Smith, D.C., McDermott, D.F., Powderly, J.D., Carvajal, R.D., Sosman, J.A., Atkins, M.B., et al. (2012). Safety, activity, and immune correlates of anti-PD-1 antibody in cancer. N. Engl. J. Med. *366*, 2443–2454.

Trumpfheller, C., Caskey, M., Nchinda, G., Longhi, M.P., Mizenina, O., Huang, Y., Schlesinger, S.J., Colonna, M., and Steinman, R.M. (2008). The microbial mimic poly IC induces durable and protective CD4+ T cell immunity together with a dendritic cell targeted vaccine. Proc. Natl. Acad. Sci. USA *105*, 2574–2579.

Wang, Z., Choi, M.K., Ban, T., Yanai, H., Negishi, H., Lu, Y., Tamura, T., Takaoka, A., Nishikura, K., and Taniguchi, T. (2008). Regulation of innate immune responses by DAI (DLM-1/ZBP1) and other DNA-sensing molecules. Proc. Natl. Acad. Sci. USA *105*, 5477–5482.

Warger, T., Osterloh, P., Rechtsteiner, G., Fassbender, M., Heib, V., Schmid, B., Schmitt, E., Schild, H., and Radsak, M.P. (2006). Synergistic activation of dendritic cells by combined Toll-like receptor ligation induces superior CTL responses in vivo. Blood *108*, 544–550.

Zhu, X., Fallert-Junecko, B.A., Fujita, M., Ueda, R., Kohanbash, G., Kastenhuber, E.R., McDonald, H.A., Liu, Y., Kalinski, P., Reinhart, T.A., et al. (2010). Poly-ICLC promotes the infiltration of effector T cells into intracranial gliomas via induction of CXCL10 in IFN-alpha and IFN-gamma dependent manners. Cancer Immunol. Immunother. *59*, 1401–1409.

Cell Reports, Volume *15*

Supplemental Information

Manipulating TLR Signaling Increases the Anti-tumor T Cell Response Induced by Viral Cancer Therapies

Juan J. Rojas, Padma Sampath, Braulio Bonilla, Alexandra Ashley, Weizhou Hou, Daniel Byrd, and Steve H. Thorne

Supplemental Figure 1

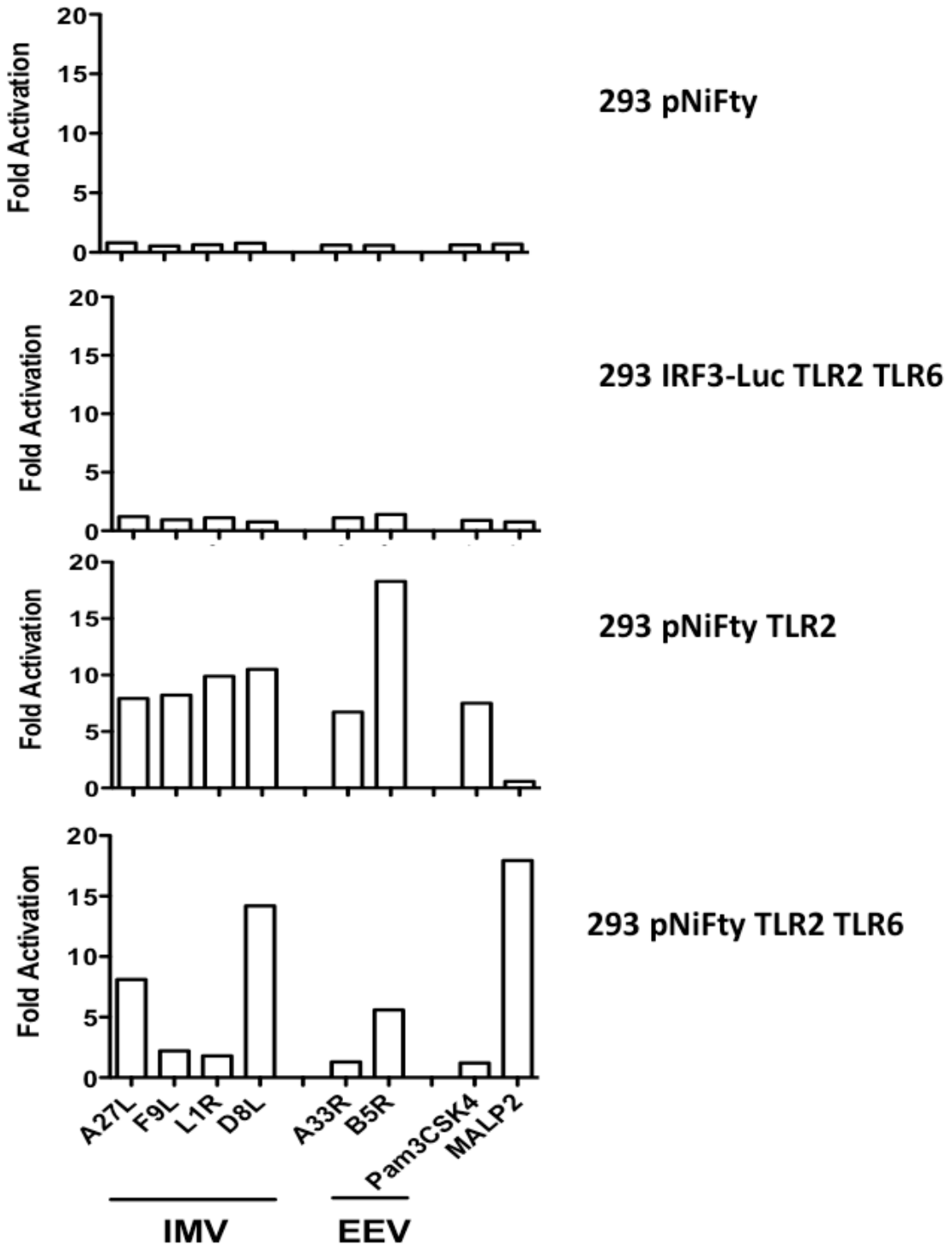

Supplementary Figure 1. Related to Figure 1. Determination of (a) TLR2:TLR6 and (b) TLR2:TLR2 activation (determined by pNiFty luciferase assay of NF-kB activation, with IRF3-luciferase assay used as a control) in 293 cells transfected to express hTLR2 or hTLR2 and hTLR6. Bioluminescence was measured by IVIS200 (Perkin Elmer) 6h after exposure to different recombinant vaccinia proteins. 293 cells not expressing any TLR were used as a control and proteins are divided into those found on the surface of either the IMV or the EEV form of the virus. PAM3CSK4 is a TLR2 homodimer ligand, and MALP2 is a ligand for TLR2:TLR6 heterodimers.

Supplementary Figure 2

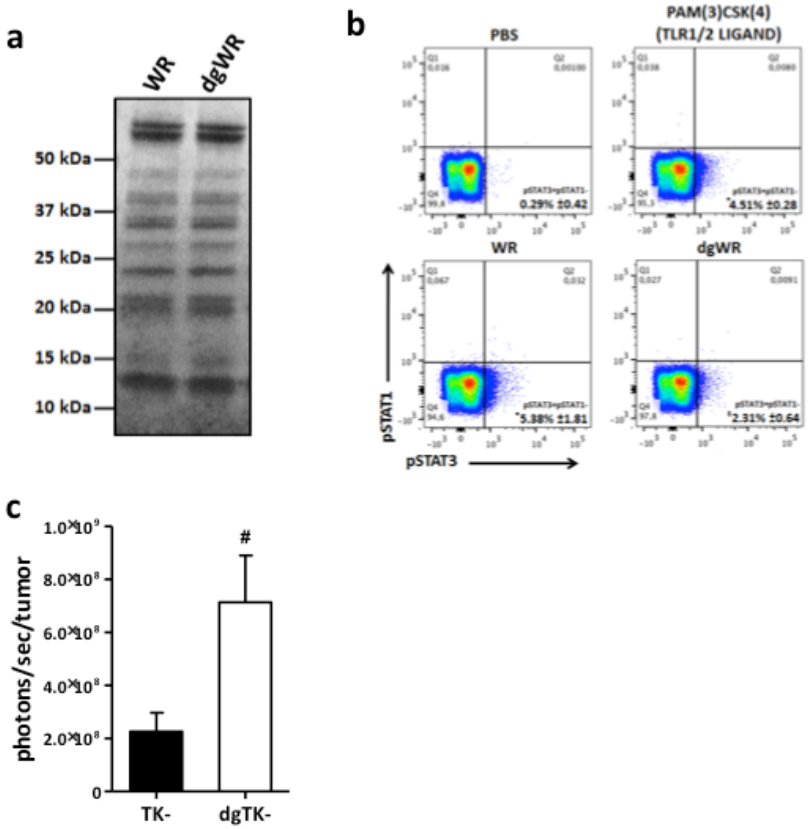

Supplementary Figure 2, Related to Figure 1. (a) Total protein content in disrupted Vaccinia virus preparations. Coomassie-blue staining was used as a control for the amount of protein loaded for blotting in figure 1a. (b) Representative distributions of pSTAT1+ and pSTAT3+ populations within splenic lymphocytes. Splenocytes from C57/BL6 mice treated as indicated were stained as in figure 1d for intracellular levels of pSTAT1 and pSTAT3 and analyzed by flow cytometry. (c) Luciferase levels from within MC38 tumors at day 3 after virus injection. C57/BL6 mice bearing subcutaneous xenografts of MC38 cells were injected intravenously with a dose of $1x10^8$ pfu per mouse of TK- or dgTK-. Viral luciferase expression was determined at day 3 after virus injection by bioluminescence imaging. Mean values of 10-12 animals +SD are plotted.

Supplementary Figure 3

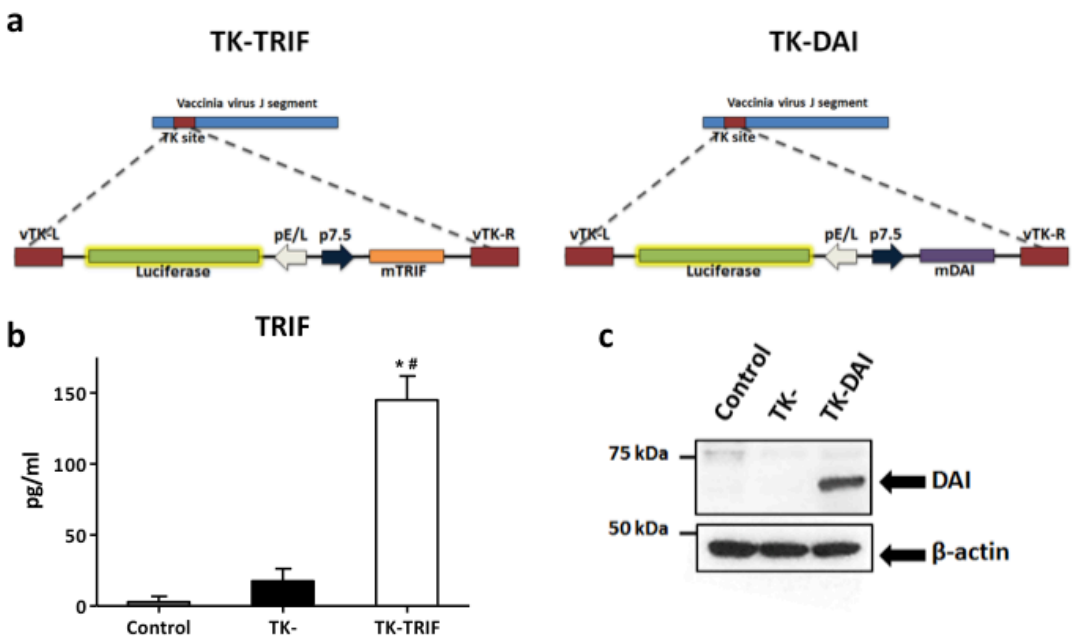

Supplementary Figure 3, Related to Figure 2. (a) Schematic diagram of TK-TRIF and TK-DAI recombinant viruses. mTRIF and mDAI, respectively, are expressed from the early/late vaccinia promoter p7.5 and cloned into the locus of the viral thymidine kinase gene. In addition, firefly luciferase gene is also expressed from the synthetic vaccinia promoter pE/L to monitor viral replication. Confirmation of mTRIF (b) and mDAI (c) expression was assessed by ELISA and Western-blot, respectively, after infection of HeLa cells (MOI of 1). *, significant $P<0.05$ compared with Control. #, significant $P<0.05$ compared with TK-.

Supplementary Figure 4

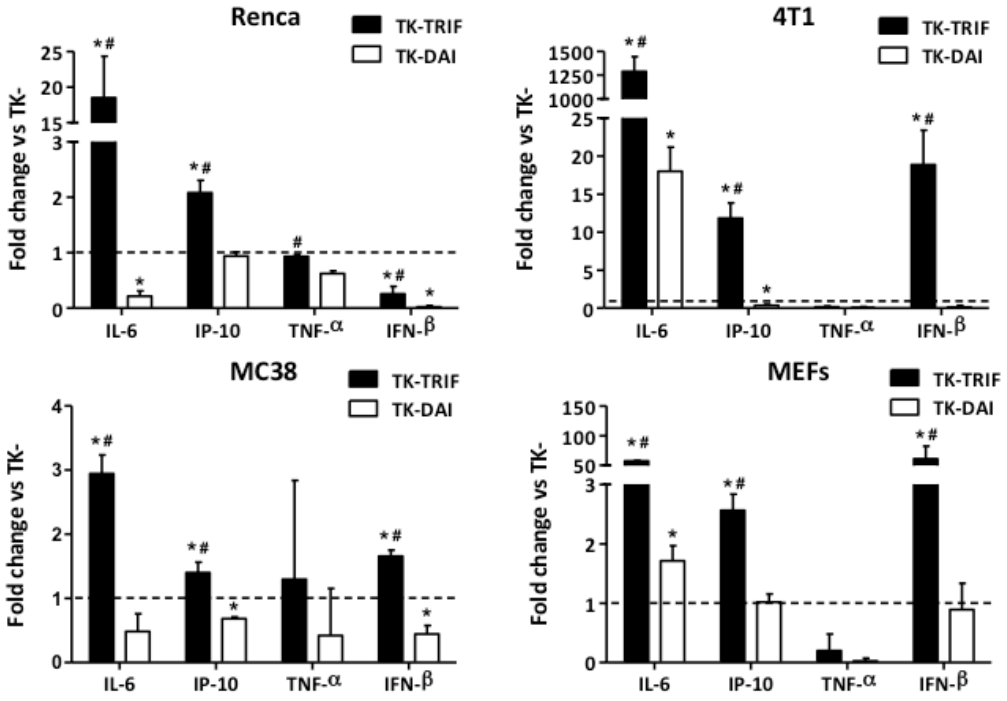

Supplementary Figure 4, related to Figure 2. Release of cytokines and chemokines *in vitro* after TK-TRIF and TK-DAI infection. IL-6, IP-10, TNF-α, and IFN-β concentrations in the supernatant of Renca, 4T1, MC38 and MEF cells were evaluated by Luminex assay 24 hours after infection with TK-, TK-TRIF and TK-DAI (MOI of 1). Data is depicted as fold change vs TK- +SD (2 independent experiments). Dashed lines indicate TK- concentrations.

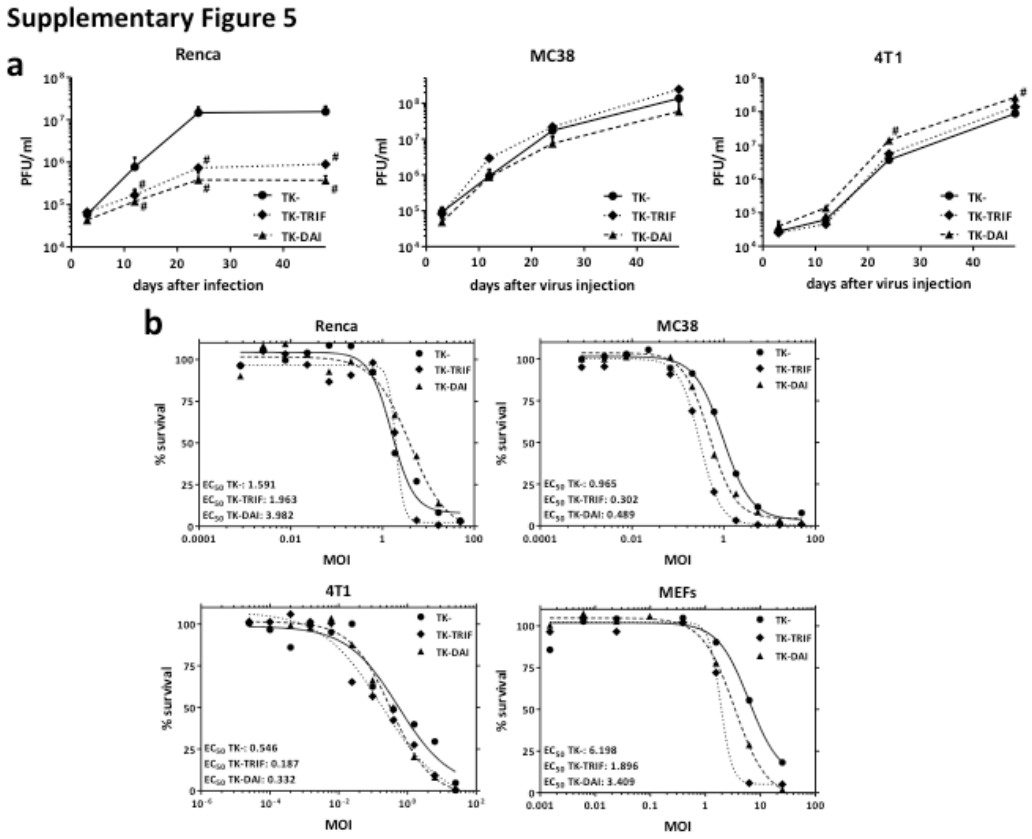

Supplementary Figure 5, related to Figure 2. (a) Viral production of TK-TRIF and TK-DAI in mouse tumor cells. Different tumor cell lines were infected with viruses at an MOI of 1 and virus production was measured by plaque-assay at different time points. Viral yield was evaluated in quadruplicate for each cell line, by carrying out two independent experiments. Means +SD are plotted. (b) Comparative cytotoxicity of TK-TRIF and TK-DAI. Cells were infected with the indicated viruses at doses ranging from 75 to 0.00025 PFU/cell. EC_{50} values (MOI required to cause a reduction of 50% in cell culture viability) at day 4 after infection are shown. Four different replicates were quantified for each cell line and mean for each MOI is depicted.

Supplementary Figure 6

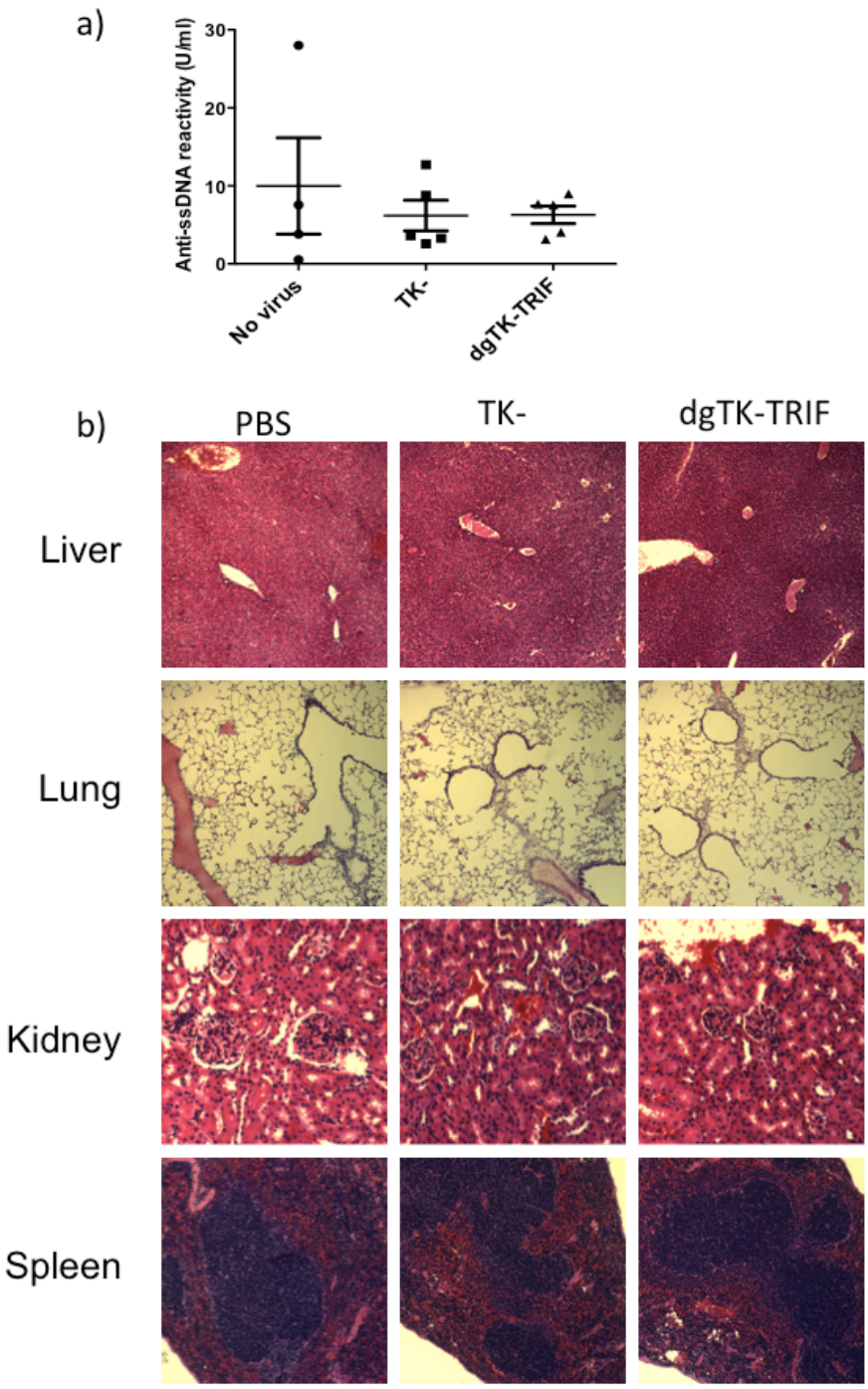

Supplementary Figure 6, related to Figure 5. BALB/c mice (n=5 per group) were treated with IV injection of PBS or 1e7 PFU of the indicated viruses. Mice were sacrificed after 21 days and (a) serum collected for quantification of the levels of circulating anti-ssDNA antibodies, and (b) other organs collected for determination of signs of toxicity and auto-immunity by H&E staining.